# Bioimpedance Parameters as a Risk Factor to Assess Pine Decay
## *An Innovative Approach to the Diagnosis of Plant Diseases*

E. Borges[1], M. Sequeira[1], André F. V. Cortez[1], H. Catarina Pereira[1], T. Pereira[1], V. Almeida[1],
T. M. Vasconcelos[2], I. M. Duarte[2], N. Nazaré[2], J. Cardoso[1] and C. Correia[1]

[1]*Instrumentation Center, Physics Department of the University of Coimbra, Rua Larga, Coimbra, Portugal*
[2]*Centro de Estudos de Recursos Naturais Ambiente e Sociedade, Escola Superior Agrária de Coimbra*
*of the Instituto Politécnico de Coimbra, Bencanta, Coimbra, Portugal*

Abstract: Electrical impedance spectroscopy, EIS, has been proving efficacy and utility in a wide range of areas, from the characterization of biological tissues to living organisms. Several commercial solutions, with high precision and resolution, are available. Nonetheless, the typical equipments are expensive, unfeasible for *in vivo* and in field applications and unspecific for concrete applications. These features, together with the lately demands in the vegetal field, fundament this work. Actually, the fast spread of asymptomatic forest diseases, with no cure available to date, such as the pinewood disease, PWD, constitute a problem of economical and forestall huge proportions. Herein is proposed a portable EIS system, for biological applications, able to perform AC current or voltage scans within a selectable frequency range. The procedure and the results obtained for a population of 24 young pine trees (*Pinus pinaster* Aiton) are also presented. Pine trees were kept in a controlled environment and were inoculated with the nematode (*Bursaphelenchus xylophilus* Nickle), that causes the PWD, and also with bark beetles (*Tomicus destruens* Wollaston). Some degree of discrimination between different physiological states was achieved. These results may constitute a first innovative approach to the diagnosis of such types of diseases.

## 1 INTRODUCTION

Electrical impedance measurements performed in a wide frequency range give rise to a great number of techniques able to characterize solids, liquids and suspensions (Callegaro, 2009). Lately, the method has proved its value also in the characterization of biological tissues and fluids, either *in vitro* or *in vivo* (Callegaro, 2009), and also to living plants (Fukuma, 2001); (Repo et al., 2000); (Väinölä and Repo, 2000); (Bauchot et al., 2000), animals (Dean et al., 2008); (Willis and Hobday, 2008) and humans (Kyle et al., 2004); (Giouvanoudi and Spyrou, 2008). Concerning the vegetal field, the applications of electrical impedance spectroscopy, EIS, techniques have been claiming significant and growing acceptance, especially as a measure of the water content in the quality control processes (Vozáry and Mészáros, 2007); (Fukuma, 2001); (Pliquett, 2010) of fruits (Fang et al., 2007) and vegetables (Hayashi

et al., 1992); (Dejmek and Miyawaki, 2002), as well as in the monitoring of the maturation process of fruits (Bauchot et al., 2000); (Harker and Maindonald, 1994) and the physiological state of living plants under adverse environmental conditions (Repo et al., 2000); (Väinölä and Repo, 2000).

The electrical impedance of a biological material, or simply bioimpedance, is a passive electrical property that measures the opposition relatively to an alternating current flow applied by an external electric field. The current I, as it passes across a section of a material of impedance Z, drops the voltage V, established between two given points of the same section, yielding the well-known generalized Ohm's law: $V=IZ$, where V and I are complex scalars and Z is the complex impedance. The law can be rewritten as $V=I|Z|e^{j\Theta}$ since, at a given frequency, the current flow I lag the voltage V by a phase of $\Theta$ (i.e. the current signal is shifted $(\Theta/2\pi)T$ s to the right with respect to the voltage

signal, in the time domain). Hence, the result of the EIS measurements is a set of complex (magnitude and phase) of impedance versus frequency.

Cell membranes, intracellular fluid (cytosol) and extracellular fluid are the major contributors of the impedance of biological tissues (Kyle et al., 2004); (Pliquett, 2010).The cytosol and the extracellular fluid are mostly constituted by water, consist in electrolytes, and act like ohmic resistors, while the insulating membranes behave like capacitors (Kyle et al., 2004); (Pliquett, 2010). It is, therefore, possible to depict the behaviour of a biological tissue by the representation of capacitive and resistive elements of a respective equivalent electrical circuit. A commonly used circuit to represent biological tissues consists of a parallel arrangement between a resistor, simulating the extracellular fluid, and a second serial arrangement connecting a resistor, this one of the cytosol, and a capacitor, of the membrane (Kyle et al., 2004) - see figure 1. Since the time constant for loading cell membranes is typically of the order of the microsecond (Pliquett, 2010), tissue impedance can be measured in a frequency range up to tens of MHz (Callegaro, 2009). In this range of frequencies the membrane performs like an almost perfect capacitor, allowing an estimation of the combined ohmic value of the cytosol and the extracellular fluid. On the other hand, using direct current level, DC, (low frequency), the current does not cross the membrane due to its insulator behaviour. This short circuit-like actuation forces the current to flow exclusively through the extracellular fluid providing, thus, a measure of its ohmic value. However, due to technical limitations and multiple dispersions ($\alpha$ dispersions at low frequencies – tissues' electrolyte behaviour – and $\gamma$ dispersions at very high frequencies – tissues' aqueous behaviour Ivorra, 2003), the usage of DC and very high frequency AC currents is restricted (Kyle et al., 2004). Therefore, it becomes quite more convenient to determine the ohmic values by prediction. The model commonly used to predict such values is the Cole bioimpedance model, in which the bioimpedance spectra is represented by means of a Cole-Cole plot (see figure 1), that explores resistance versus reactance, allowing the determination of the ohmic values of the cytosol and the extracellular fluid. The mathematical expression descriptive of the Cole-Cole plots is the Cole equation (here expressed has in Grimnes and Martinsen, 2008):

$$Z = Z_\infty + \frac{\Delta R}{1 + (j\omega\tau)^\alpha}, \quad \Delta R = R_0 - R_\infty \quad (1)$$

Where $Z$ is the impedance value at frequency $\omega$

(with $\omega = 2\pi f$), $Z_\infty$ is the impedance at infinite frequency (high frequencies) (note: this term is misleading and is replaced by an ideal resistor $R_\infty$), j is the complex number, $R_0$ is the impedance at DC frequency, $\tau$ is the characteristic time constant and $\alpha$ is a dimensionless parameter with a value between 0 and 1.
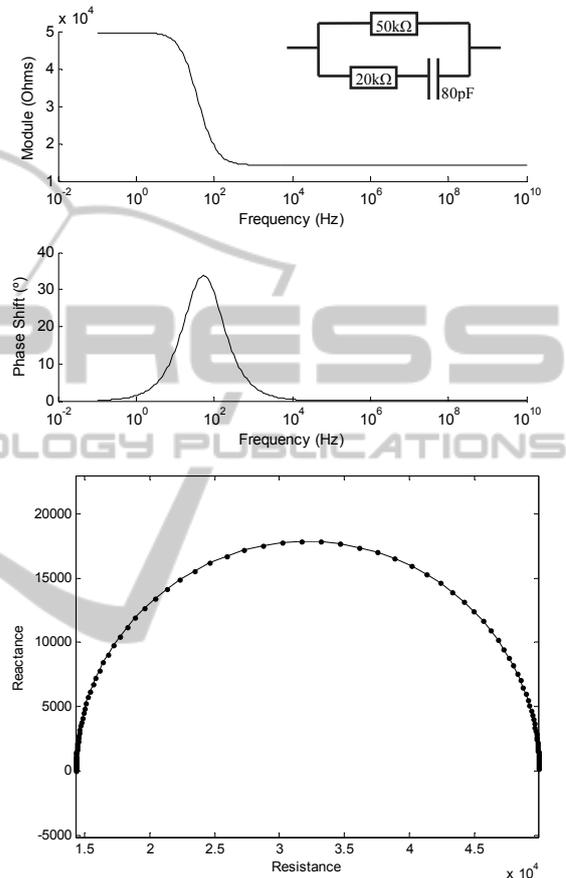


Figure 1: Bode and Cole-Cole diagrams obtained by simulation with Matlab® for an electrical circuit representing a hypothetical biological tissue (right top of the figure).

The relationship between reactance and resistance, perceived in a Cole-Cole plot, expresses the electrical properties of tissues. Diseases and nutritional or hydration levels may change their physiological state. These changes have direct influence in the impedance spectra. The phase angle and other interrelated indices, such as $Z_0/Z_\infty$ (Kyle et al., 2004) and $Z_0/Z_{50}$ (Hayashi et al., 1992), have been used to extract information about the physiological condition of biological materials. The index $Z_0/Z_{50}$ gains some significance since it is at the 50 kHz that the current starts passing through both cytosol/membranes and extracellular fluid, although

the proportion varies from tissue to tissue (Kyle et al., 2004).

The nature of the impedance excitation signal varies depending on the application. It is possible to excite the sample with a current and measure a voltage or to do the exact opposite. The discussion on what source, voltage or current, is the most convenient remains. Current sources, CS, provide suitably controlled means of current injection (Rafiei-Naeini et al., 2007) and present reduced noise due to spatial variation when compared with voltage sources, VS (Ross et al., 2003). However, CS accuracy decreases with high frequency (Yoo et al., 2010), especially due to their output impedance degradation (Ross et al., 2003). Since the impedance measurements are limited to field strength where the current is linear with respect to the voltage applied (Pliquett, 2010), or vice-versa, CS need high-precision components (Saulnier et al., 2006) and a limited bandwidth operation range (Yoo et al., 2010, Saulnier et al., 2006) to overcome the stated limitation. On the other hand, VS, although producing less optimal EIS systems (Saulnier et al., 2006), can operate over a sufficient broad frequency range (Yoo et al., 2010); (Saulnier et al., 2006) and are built with less expensive components (Saulnier et al., 2006).

Nowadays, instruments with high precision, high resolution and frequency ranges extending from some Hz to tens of MHz are commercially available (Callegaro, 2009). However, in what concerns to the range of low or high frequencies (already above 100 kHz), the degradation of the excitation signal affects the accuracy of the measurements (Callegaro, 2009). Besides, the typical solutions consist in impedance analyzers and LCR meters which are desktop instruments (Callegaro, 2009), unfeasible for *in vivo* (Callegaro, 2009) and in field applications.

Those EIS features, together with the lately demand in the vegetal applications, fundament this work. In fact, there are several plant pest and diseases affecting different cultures of huge economic and forestall importance, not only in our country but also around the world. This is the case of esca disease in vineyard, ink disease in chestnuts or pinewood disease, PWD, and bark beetles in pinus stands, among others. It is known that PWD, the case study presented in this paper, is caused by the nematode *Bursaphelenchus xylophilus* Nickle, that is housed in the tracheas of pine sawyer *Monochamus galloprovincialis* Olivier. Bark beetles in general and pine shoot beetle (*Tomicus destruens* Wollaston), in particular, play an important role in nematode establishment since they are responsible

of pine decay, condition required for *M. galloprovincialis* oviposition. The PWD disease leads to a rotting process from within the plant (therefore, inside the stem) so that symptoms are difficult to see from the outside. Furthermore, there is still no cure available and the only solution to discontinue the progress of the disease throughout the culture is to identify and isolate the specimens that seem to have contracted the disease.

The authors propose a portable EIS system able to perform AC scans within a selectable frequency range. The system implements the phase sensitive detection, PSD, method and can drive either a current or a voltage signal to excite a biological sample in field or *in vivo*. The instrumentation was designed to be cost-effective and usable in several applications.

The design specifications are listed in Table I.

Table 1: Summary of specifications of the EIS system.

| Parameter | Range | |
|---|---|---|
| | Current Mode | Voltage Mode |
| Measuring method | 2 electrodes | |
| Frequency | 1 kHz to 1 MHz | |
| Signal amplitude | 25 uA | 4.6 V |
| Impedance magnitude | 100 $\Omega$ to 100 k$\Omega$ [1] | 1.5k $\Omega$ to 2.2 M$\Omega$[1] |
| Impedance phase | -$\pi$ rad to $\pi$ rad | -$\pi$ rad to $\pi$ rad |
| Mean absolute magnitude error | 1675.45 $\Omega$ | 709.37 $\Omega$ |
| Mean absolute phase error | 2.45 % | 2.06 % |
| Mean distortion | 0.29 % | 0.48 % |
| Mean SNR | 117.0 dB | 118.8 dB |
| Calibration | Automatically calibrated by software | |

A first interesting case study is presented for a population of 24 young pine trees (*Pinus pinaster* Aiton), from a controlled environment. Pine trees were inoculated with the nematode that causes the PWD and also with bark beetles (*T. destruens* Wollaston).

## 2 SYSTEM DESIGN

### 2.1 General Description

The developed EIS system employs two electrodes and consists of three main modules: signal conditioning unit, acquisition system (PicoScope® 3205A) and a laptop for data processing (Matlab® based software), as figure 2 depicts. There were built two different versions: one OEM for lab studies and another miniaturized version for field acquisitions.

The electrodes being used are beryllium cooper gold platted needles with around 1.02 mm in

diameter. The bioimpedance measurement requires the most superficial possible penetration of the electrodes in order to reduce the dispersion of the needles surface current density (Grimnes and Martinsen, 2008), and also to reduce damage on the biologic sample.
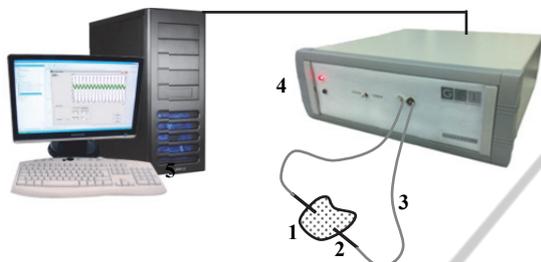


Figure 2: Schematics of the EIS OEM system – 1) Biologic sample; 2) electrodes; 3) short coaxial cables; 4) EIS system conditioning unit and acquisition system, with the Picoscope®3205A incorporated; 5) laptop/PC.

The digital oscilloscope PicoScope® 3205A has dual functionality: 1) synthesizes and provides the excitation AC signal to the conditioning unit (ADC function); 2) digitizes both excitation and induction signals at high sampling rates (12.5 MSps) and transfers data to the computer via USB where it is stored. The signal conditioning unit receives the exciting AC signal, coming from the PicoScope®, and amplifies it to be applied, through an electrode, to the specimen under study. The induced AC signal is collected by a second electrode and is redirected to the conditioning unit where it is also amplified. Both excitation and induced signals are conduced to the PicoScope® to be digitized.

It is also important to remark that the conditioning unit has an external switch that allows the user to select the mode type of excitation: by AC current or AC voltage. As previously mentioned, it is more advantageous to choose a mode of excitation over another, depending on the type of application.

The features of both excitation modes are described below.

## 2.2 Design Specifications

The current mode circuit employs the current-feedback amplifier AD844 in a non-inverting ac-coupled CS configuration (see figure 3), already studied by Seoane et al., 2006.

A common problem inherent to bioimpedance measurements is the charging of the dc-blocking capacitor between the source and the electrode due to residual DC currents (Seoane et al., 2006). This effect lead to saturation of the transimpedance

output of the AD844. The DC feedback of the implemented configuration maintains dc voltage at the output close to 0V without reducing the output impedance of the source. Subsequently, the output current, is maintained almost constant over a wide range of frequencies.
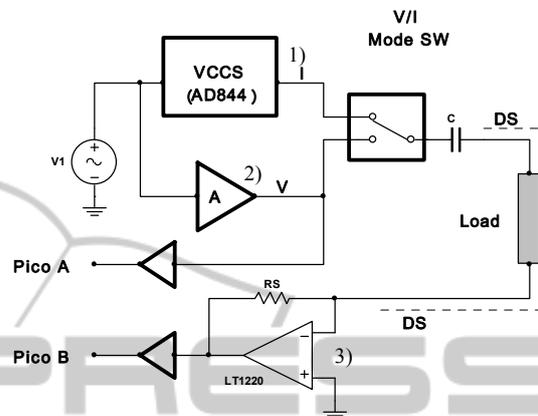


Figure 3: Schematic of the EIS system conditioning unit - 1) AC current source; 2) AC voltage source; 3) current/voltage sense.

The high speed voltage-feedback amplifier LM7171 is employed in the voltage mode circuit (see figure 3). This behaves like a current-feedback amplifier due to its high slew rate, wide unit-gain bandwidth and low current consumption. Nevertheless it can be applied in all traditional voltage-feedback amplifier configurations, as the one used. These characteristics allow the maintenance of an almost constant voltage output over a wide range of frequencies.

Current or voltage signals resulting from voltage or current excitation modes, respectively, are sensed by a high speed operational amplifier, LT1220 (see figure 3), which performs reduced input offset voltage and is able of driving large capacitive loads.

Gain values of both current excitation source and voltage excitation source can be changed in order to extend the range of impedance magnitude. The transductance gain of the LT1220 is currently set to 5.1 kΩ and defines the gain of the system. Since the gain values are known and also the amplitude of the AC excitation signal, $V_{sin}$, from the PicoScope®, the EIS system is calibrated automatically by software.

## 2.3 Cables Capacitance

The characteristics of the cables that connect between the conditioning unit and the sample under study are also crucial. For an optimized signal-to-noise ratio, coaxial cable must be used.

Nevertheless, this type of cable is prone to introduce high equivalent parasitic capacitances, which translate in errors in the bioimpedance measurements, especially at high frequencies. To overcome this effect, the employed RG174 RF coaxial cables (capacitance of 100 pF.m-1) are as short as possible (around 15cm). It was also implemented a driven shield technique to the coaxial cables, which permits to partially cancel the capacitive effect, that otherwise is generated between the internal and the external conductors, by putting both at the same voltage (Yamamoto et al, 1985). Reductions in the capacitive effect of 20.4%, in the current mode, and around 35.8%, in the voltage mode, at the highest frequencies are verified. Figure 4 depicts the capacitive effect reduction by the usage of the driven shield technique.
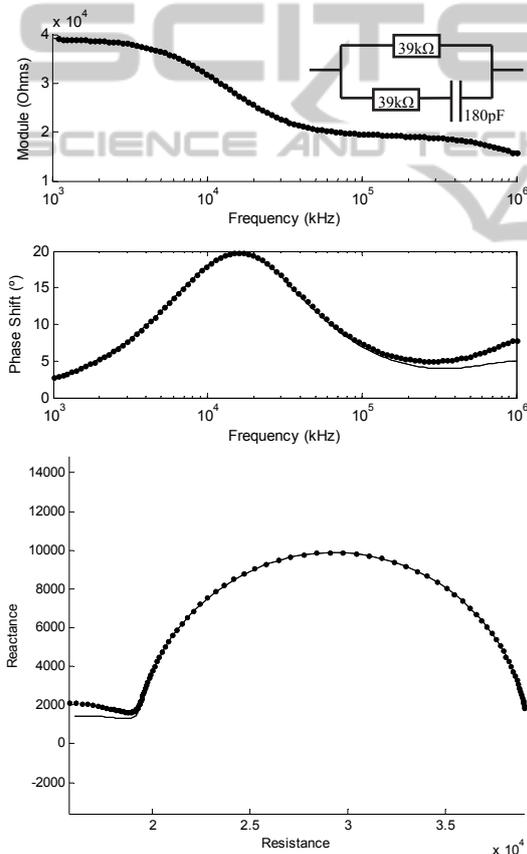


Figure 4: Bode and Cole-Cole diagram showing the reduction of cables capacitive effect by the application of the driven shield technique. The voltage mode excitation was used to analyze the circuit at the right top. The reduction is more noticeable at high frequencies where the capacitive effects have more influence.

When assessing bioimpedance, the capacitive effects from cables are not the only exerting influence. In fact, phase shift effects, perceptible especially in the high frequencies range, are introduced mainly by the amplifiers. The influence of phase shift errors has a cumulative effect that is translated, in the impedance spectra, as an inflexion that occurs at high frequencies (see figure 4).

This behaviour can be simulated by an equivalent circuit as it is like the system analyzes any load always in parallel with a capacitor.

The impedance magnitude, at high frequencies, is also affected. It presents a characteristic decline as the bode diagrams of the figure 4 show. In the developed EIS system, the slight decline of the impedance magnitude is due to the loss of the product gain-bandwidth of the LT1220 for high frequencies.

Since stray capacitances are considered systematic errors of the system, thus affecting all the measurements, theirs influence doesn't directly affect the results. Although, it is convenient to have an approached sense of the real equivalent circuit (see figure 5), in such a way that the effect of all the parasitic elements can be considered and/or discounted where justified.
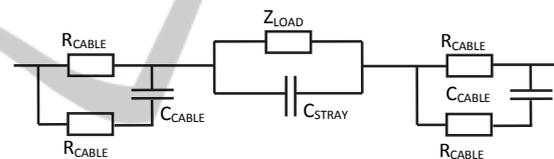


Figure 5: Equivalent electric circuit of all parasitic elements affecting impedance measurements of a load, $Z_{LOAD}$. The effect of the stray capacitances from cables, $C_{CABLE}$, is minimized by the driven shield. Other stray capacitance effect, $C_{STRAY}$, due primarily to the phase shift of amplifiers, can be minimized by software.

# 3 SOFTWARE AND ANALYSIS PROCESSING

## 3.1 General Specifications

The software interface, developed with Matlab® tools, allows the operator to choose the parameters of the bioimpedance analysis and to monitor the data acquisition. The operator can perform an analysis for one specific frequency or alternatively can carry out a true bioimpedance spectroscopy. These two software functioning modes can be programmed for continuous monitoring, where the number of acquisitions and the intervals between them are specified by the user. The interface includes a basic function that allows a preview of the Bode and Cole-

Cole diagrams of the acquired data. Bioimpedance *txt or *mat files are saved in a pre-determined directory with a filename, previously chose by the user, to which date and time are associated. Each file contains information about magnitude, phase shift and real and imaginary parts of the measured impedance, for each frequency.

The type of bioimpedance spectroscopy implemented consists in a frequency AC sweep, whose limit values are 1 kHz and 1 MHz. Notwithstanding, the software allows the operator to choose other frequency limits, as well as the number of intervals between them. In addition, it can be choose a linear or logarithmic analysis. Therefore, the frequencies, f(i), over which the impedance of a sample is analysed, are determined by the following equations:

For a linear analysis:

$$f(i) = f\_start + i * \frac{f\_stop - f\_start}{n - 1},$$

$$\forall\, i \subset [0, n-1] \wedge n \in N \qquad (2)$$

For a logarithmic analysis:

$$f(i) = f\_start * \left[ 10^{\frac{\log_{10}\left(\frac{f\_stop}{f\_start}\right)}{(n-1)}} \right]^i,$$

$$\forall\, i \subset [0, n-1] \wedge n \in N \qquad (3)$$

Where f_star and f_stop are, respectively, the first and final frequencies of the AC sweep, and n the number of intervals between them.

## 3.2 PSD Method

To assess the impedance phase shift it is implemented a digital Phase Sensitive Detection, PSD, method with a novel implication. As stated in the literature, the PSD method is a quadrature demodulation technique that implements a coherent phase demodulation of two reference (matched in phase and quadrature) signals (He et al, 2008); (Dobrev et al., 2008). It is also known that this method is preferable over others especially when signals are affected by noise (Dobrev et al., 2008).

The signal from the Picoscope® that corresponds to the current, $V_I = B\sin(\omega t + \varphi_2)$, is set as the reference signal. Since the phase of the signal $V_I$ is not controlled, it is easily understandable that it doesn't necessarily contain a null phase. This statement remains valid whether $V_I$ is used to excite the sample, in the current mode, or whether it corresponds to the current passing through the sample, in the voltage mode. The signal from the

Picoscope® that corresponds to the voltage, $V_V = A\sin(\omega t + \varphi_1)$, also contains a non-null phase. Both amplitudes, A and B, are also different from each other and none equals to 1.

The developed PSD algorithm was tested with Matlab® for several phases and amplitudes without the theoretical requirements (i.e., ensure that the reference signal has null phase at the origin and that its amplitude equals to 1 (He et al., 2008)). For all of them it was showed an always corrected phase shift assessment, when compared to the results obtained for a reference signal with the theoretical characteristics.

In addition, the mathematical resolution for the demodulation of two signals with non-null phases and amplitudes not equal to 1, corresponds to the phase difference between both signals. The following mathematical demonstration and the schematic block diagram (shown in figure 6) support the results obtained with the simulation.

Assuming that the analog input signals $V_V(t)$ and $V_I(t)$ are sine waves of frequency f, amplitude A and B, respectively, and initial phase $\varphi_1$ and $\varphi_2$, respectively:

$$V_V(t) = A \sin(2\pi f + \varphi_1) \qquad (4)$$

$$V_I(t) = B \sin(2\pi f + \varphi_2) \qquad (5)$$

The digitized input signals $V_V(n)$ and $V_I(n)$ are obtained from $V_V(t)$ and $V_I(t)$, respectively, by sampling at a frequency $f_s$, where $f_s$ is a multiple of the f:

$$V_V(n) = A \sin\left(\frac{2\pi f n}{f_s} + \varphi_1\right), n \in [0, N-1] \qquad (6)$$

$$V_I(n) = B \sin\left(\frac{2\pi f n}{f_s} + \varphi_2\right), n \in [0, N-1] \qquad (7)$$

Where N is the number of samples. $N/f_s$ is the measurement time and must be an exact multiple of $1/f$, so that there is whole number of cycles of the sine wave.
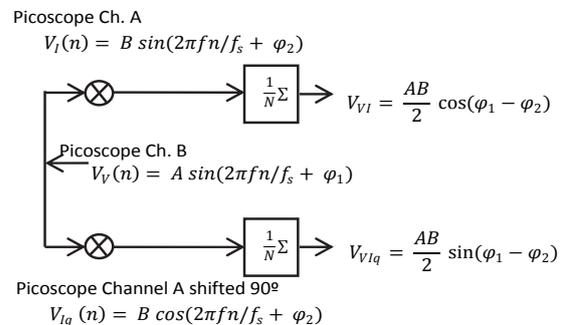


Figure 6: Schematic of Phase-sensitive Demodulator implemented in the EIS system.

The signal $V_I(n)$ is set as reference. The quadrature reference signal, $V_{Iq}(n)$, results from the reference signal shifted by a phase of 90°. Consequently, $V_{Iq}(n)$ is cosine with the same frequency, amplitude and initial phase as $V_V(n)$:

$$V_I(n) = B \sin\left(\frac{2\pi f n}{f_s} + \varphi_2\right), n \in [0, N-1] \quad (8)$$

$$V_{Iq}(n) = B \cos\left(\frac{2\pi f n}{f_s} + \varphi_2\right), n \in [0, N-1] \quad (9)$$

The output voltages of the system shown at figure 6 are:

$$V_{VI} = \frac{1}{N} \sum_{n=0}^{N} V_V(n)\, V_I(n) \quad (10)$$

$$V_{VIq} = \frac{1}{N} \sum_{n=0}^{N} V_V(n)\, V_{Iq}(n) \quad (11)$$

The multiplication between two sine signals, with the same frequency, results in a sum of a DC signal and a sine signal with a frequency that is the double of the original. The double frequency component can be suppressed since the time is a multiple of the period of the input sine signal. Therefore, it remains only the DC component which amplitude is dependent on the amplitude of the individual sine signals and their relative phase:

$$V_{VI} = \frac{AB}{2} \cos(\varphi_1 - \varphi_2) \quad (12)$$

$$V_{VIq} = \frac{AB}{2} \sin(\varphi_1 - \varphi_2) \quad (13)$$

From the expressions above, the resulting amplitude and phase can be determined:

$$\varphi_1 - \varphi_2 = \arctan\left(\frac{V_{VIq}}{V_{VI}}\right) \quad (14)$$

$$A = \frac{2}{B} \sqrt{(V_{VI})^2 + (V_{VIq})^2} \quad (15)$$

The determined phase is actually a phase difference between the demodulated signal, $V_V$ and the reference signal, $V_I$, i.e., it corresponds to the phase difference between voltage and current signals. Figure 7 shows the consistence of the algorithm when the impedance phase of a real data is compared with a spice simulation in Cadence®.

The determination of impedance magnitude cannot be achieved by the PSD method, since the amplitude equation (equation 15) shows a dependence on the amplitude of the reference signal, which, in this case, is not equal to 1. Hence, to assess amplitude, the EIS system algorithm processes the root mean square, RMS, of both signals $V_V(t)$ and $V_I(t)$ from de channel B and A, respectively, of the Picoscope®. In this manner, the impedance magnitude is given by the ratio between the RMS value of the signal $V_V(t)$ and the rms value of the signal $V_I(t)$:

$$|Z| = \sqrt{\frac{\sum_{i=0}^{N} (V_V{}^2)_i}{\sum_{i=0}^{N} (V_I{}^2)_i}}\; Gain\;, \qquad \forall\, i \in [0, N-1] \quad (16)$$

Where *Gain* is the EIS system gain defined by the transconductance gain of the LT1220 (see section 2.2).
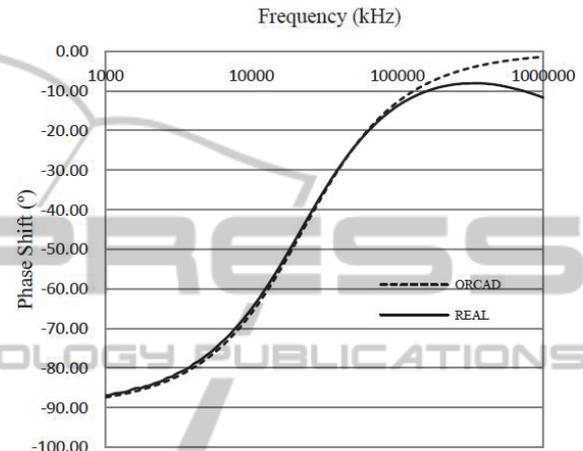


Figure 7: Comparison between impedance phase of a real data and Cadence® simulated data for a RC circuit. The deviation that occurs between the graphics, at high frequencies, is due to the influence of stray capacitances (see section 2).

# 4 BIOLOGIC APPLICATION STUDY

## 4.1 Materials and Methods

Twenty four young healthy pine trees (*Pinus pinaster* Aiton), with about 2,5 meters tall and 2 to 3 centimetres in diameter, constituted the population for the conducted study. The pine trees were placed in vases in a controlled water environment at a greenhouse. Half of the tree population was watered during 5 minutes per day (~ 133,37 mL/day), while the other half were watered during only 2 minutes per day (~ 66,67 mL/day). This second half was less watered to maintain a relevant level of hydric stress.

After one month elapsed since the pine trees were placed in the greenhouse, the inoculations with pinewood nematode, PWN, (*Bursaphelenchus xylophilus* Nickle) and with the bark beetle (*T. destruens* Wollaston) were performed. Six pines were inoculated with PWN, other 6 pines were

inoculated with bark beetles, other 6 pines were inoculated simultaneously with PWN and bark beetles, while the remaining 6 were kept under normal conditions, i.e., healthy. The position of the pines in the greenhouse was made so that each sub-group had the same number of pines with normal watering (5 min/day) and with reduced watering (2 min/day).

To perform the inoculations with bark beetles, callow adults were collected immediately after emergence. In each tree, a box containing 15 beetles were placed in the middle and the device was covered using Lutrasil tissue to avoid beetles escape.

The inoculation with the PWN followed an innovative approach. Firstly, three 2 x 2 cm rectangle of cork were removed from the first tiers of the trunk (about 1,80 m above the soil) and exposed phloem was erased with a scalpel in order to increase the adhesion of the PWN. Afterward, 0,05 mL of of a PWN suspension was placed on in each incision. In the total, 6000 nematodes were inoculated per tree. To finalize the task, the removed rectangle of cork was fixed in the respective place and wrapped with plastic tape.

Seventy days after the inoculations, the EIS measurements were performed in all the tree population. At this time, the pine trees inoculated with PWN presented some visually symptoms of the PWD. The decay of those trees, rounded 40 %. Two of the healthy pines died (decay of 100 %) due to hydric stress. All remaining individual appeared healthy.

To perform the EIS measurements, the electrodes were placed in the trunk of each tree, in a diametric position, and about 30 cm above the soil. It was used the portable EIS system version in the voltage mode of excitation and a frequency range between 1 kHz and 1 MHz. There were taken two measurements for each tree. The acquisitions took place between 11 a.m. and 13 p.m. since it was already verified in previous studies that at this time period the trees impedance is higher and presents few variation (see figure 8 – section 4.2).

In order to relate the EIS data with the PWD and the stage of the disease, the trunk of the pine trees inoculated with PWN were cut in three distinct regions to perform a count of nematodes. The cuts were executed: a) immediately below the inoculation incision (180 cm above the soil); b) 30 cm above the soil (where EIS measurements took place); and c) in the middle of the previous two cuts (approximately 80 cm above the soil).

After the EIS measurements, two healthy pines were monitored by two independent portable EIS

systems. After a week of monitoring, the same pines were inoculated with PWN, and the measurements continued during 7 more weeks. The main purpose of this last experiment was to study the variation of the pine EIS profiles during the decay due to the PWD.

## 4.2 Results

For each obtained impedance spectra there were assessed several impedance parameters. Due to paper space limitation and also because it is a well-known impedance parameter, it will only be presented the results obtained for the ratio $Z_1/Z_{50}$. Note that it is used the index 1, that corresponds to the lowest analyzed frequency (1 kHz), instead of the index 0, as explained in section 1.

### 4.2.1 Impedance Daily Oscillation

The EIS measurements revealed that EIS Cole profiles have a daily oscillation. To analyze this behavior it was calculated the $R_1/R_{50}$ ratio (R represents module) for a period of 4 days.
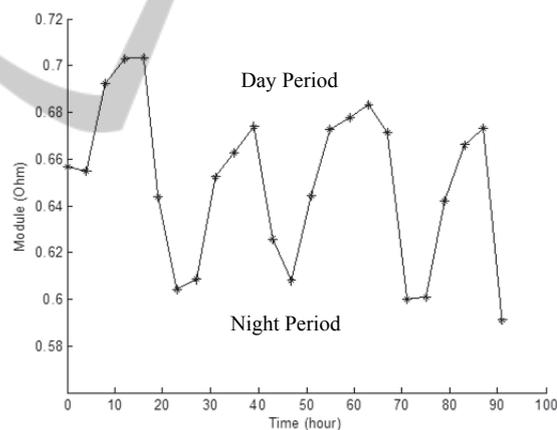


Figure 8: Variation of the $R_1/R_{50}$ ratio during the monitoring of a healthy pine tree. The impedance values show a daily oscillation that is characteristic of the studied trees.

To confirm the daily oscillation it was calculated the fast fourier transform of this ratio. A frequency of 11,57 µHz was clearly founded, which corresponds to a frequency of 24 h.

The lower values of the ratio $R_1/R_{50}$ correspond to the night period, while the higher values correspond to the day period where the temperature and luminance are higher (between 11 a.m. and 15 p.m.). Previous studies on plants also shown that, during the day period, the variation of impedance values is lower than the one observed at the night

period. This was the main reason that lead to performing the EIS measurements between the 11 a.m. and 14 p.m.

### 4.2.2 Discrimination between Physiological States

In order to compare results between the different physiological states of the trees, there were assessed several impedance parameters. The impedance parameter that showed better results was the $Z_1/Z_{50}$ ratio – see figure 9.
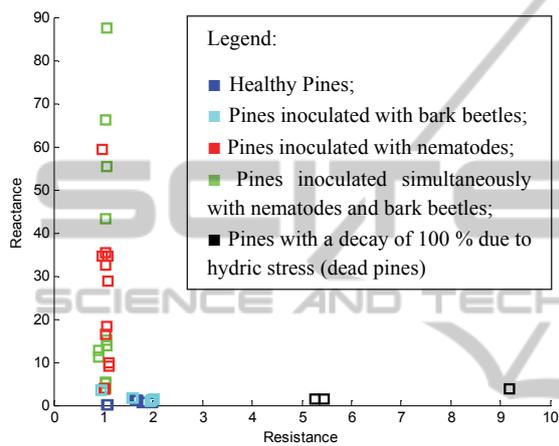


Figure 9: Values of the impedance parameter $Z_1/Z_{50}$ for each of the 24 pine trees. Note that there are represented two values for each pine.

The analysis of the obtained results shown that the healthy pines and the pines inoculated with bark beetles have similar $Z_1/Z_{50}$ values. In fact, the bark beetles doesn't damage the inner structure of the trees, therefore it was expected that the impedance profiles were similar between healthy pines and pines inoculated with bark beetles.

On the other hand, $Z_1/Z_{50}$ values for the pines inoculated with nematodes and also, for those inoculated simultaneously with nematodes and bark beetles, locates in the same region, different from the previous one, of the graph of figure 9. Those values present a relatively high dispersion in terms of reactance. It was later confirmed that higher reactance $Z_1/Z_{50}$ values correspond to higher number of nematodes in the tree (see figure 10 from section 4.2.3).

The pines that died due to hydric stress (decay of 100%) were also studied and the $Z_1/Z_{50}$ parameter present high resistance values in relation to all the other pines.

### 4.2.3 Relation between the Number of Nematodes and Impedance Parameters

The counting of nematodes in the several cut sections revealed that the concentration of nematodes was higher in the cut sections b) and c) for the pines less watered (pines 1, 2 and 3) – see table 2. It is known that the nematodes move toward watered regions along the trunk. For this reason, the concentration of nematodes in the lower parts of the trunks was much higher for the pines with less watering than for those with regular watering (pines 4, 5 and 6).

Table 2: Number of nematodes in the trunks of pine trees per cut sections.

| Tree | Cut Section | Number of nematodes in 0,05 mL |
|---|---|---|
| 1 | a | 1 |
| | b | 0 |
| | c | 133 |
| 2 | a | 0 |
| | b | 43 |
| | c | 1 |
| 3 | a | 0 |
| | b | 0 |
| | c | 112 |
| 4 | a | 4 |
| | b | 20 |
| | c | 0 |
| 5 | a | 0 |
| | b | 17 |
| | c | 0 |
| 6 | a | 0 |
| | b | 0 |
| | c | 14 |
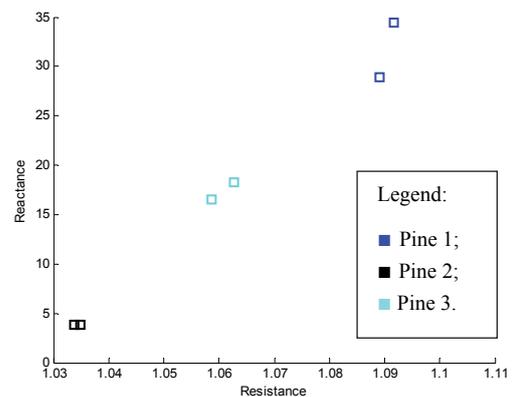


Figure 10: Values of the impedance parameter $Z_1/Z_{50}$ for the pines inoculated with nematodes and with low watering (pines 1, 2 and 3 from the table 2). Note that there are represented two values for each pine.

These results for the nematodes counting support the already referred results obtained for the $Z_1/Z_{50}$ impedance parameter. In fact, it is observed a clear

relation between the number of nematodes and the reactance dispersion for the $Z_1/Z_{50}$ parameter, as figure 10 shows. The higher the number of nematodes is, the higher is the reactance value of $Z_1/Z_{50}$. It is considered that the dispersion in terms of resistance is not significant when compared with values from pines in other physiological condition – see figure 9 from section 4.2.2.

### 4.2.4 EIS Monitoring during Pine Decay

There were monitored two healthy pines, one with low watering (2 min/day) and another with regular watering (5 min/day). After one week from the beginning of the monitoring, both pines were inoculated with nematodes. It was shown again a dispersion of the reactance values of the $Z_1/Z_{50}$ parameter, as figure 11 shows. As time passed the reactance values became higher. The higher values of reactance were achieved for the pine with less watering. According to the previous presented results, it was expected that the number of nematodes increase in the below part of the trunk for the pines with less watering; and consequently, to observe a higher rising of the reactance of the $Z_1/Z_{50}$ parameter. After the 6th week, pines start to decay strongly and it was observed a relevant decrease of the reactance and a significant increase of the resistance for the same parameter – see figure 11. The higher values of resistance were achieved for the pine with less watering, and also in a shorter period of time. At the end of the monitoring, the decay of the pines, evaluated by an expertise, was about 80 % for the pine with regular watering and 100 % for the pine with less watering.

From the figure 11 b), that represents a closer view of the $Z_1/Z_{50}$ values for the monitoring, it is possible to observe that the path followed during the period of nematodes population increasing is different from the path followed during the period of decay, i.e., it is observed an hysteresis-like behavior.

## 5 CONCLUSIONS

The EIS system was developed in order to ensure a robust, efficient and fast bioimpedance analysis. The adaptability to different biological applications, the portability and the usage of easily accessible and affordable components, were preferred aspects taken into account. In this manner, the system allows the user to choose the settings of the analysis that best fit to a specific application. Furthermore, there were built two versions of the equipment: one OEM

version for lab tests and a miniaturized version for field applications.
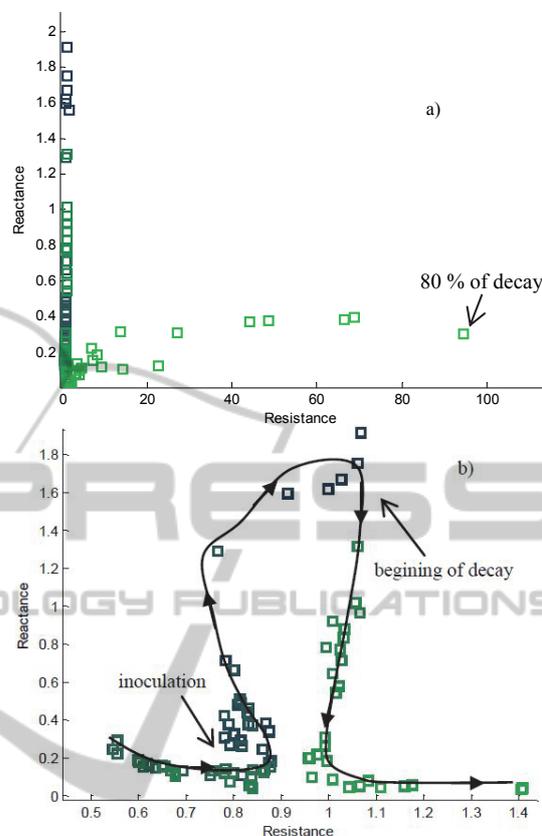


Figure 11: a) Evolution of the Z1/Z50 during the monitoring time (8 weeks). b) Closer view from the $Z_1/Z_{50}$ evolution, showing a hysteresis-like behaviour.

The system is able to perform AC scans within a frequency range from 1 kHz to 1 MHz. The frequency limits and the number of intervals of the scan can be selected at the user interface (developed with Matlab® tools). The type of signal used to excite de sample, voltage or current, can be preselected by an external switch. This allows the usage of the source with the best behaviour in a concrete application.

The implemented PSD algorithm allows a very good phase shift assessment without the need to use a reference signal of amplitude equal to 1 and null-phase at the origin. In fact, the signal set as reference has undetermined phase and amplitude. All the algorithm tests revealed results analogous to the theoretical.

To overcome problems inherent to stray capacitive effects from cables, a driven shield technique is applied. The maximum phase shift reduction is estimated at 20.4 % for the current

excitation mode and at 35.8% for the voltage mode.

The biological application study aimed at discriminating between different pine tree physiological states.

The obtained results suggest that the implemented method may constitute a first innovative approach to the early diagnosis of plant diseases. In fact, the achieved impedance parameters allow discriminating three different physiological states: healthy trees, trees with PWD and trees in hydric stress.

The trees with PWD present $Z_1/Z_{50}$ ratio with high values of reactance, suggesting that the current flows preferably trough the cytosol. In fact, the action of the nematodes inside the tree may destroy cell membranes. This means that membranes capacitor effect becomes less significant in the impedance measurement.

It was also shown that the number of nematodes and $Z_1/Z_{50}$ impedance parameter are related. The higher the number of nematodes is, the higher the reactance of the ratio is.

The action of bark beetles seems not to interfere, at least in measurable terms, in the level of hydric stress of pine trees.

Healthy trees, with high values of hydric stress (decays above 80 %), and also trees with PWD at advanced stages, revealed low reactance and high resistance for the same studied parameter. The high values of resistance are justified due to the water loss in the tree. Consequently, it means that for this specific case, the method cannot distinguish between trees with PWD or trees with high level of hydric stress but with no disease. However, it is known that advanced stages of PWD promote high levels of hydric stress. This means that both cases represent, in practical terms, the same situation, i.e., the tree presents high probability to die. In addition, in the stages where the method is able to distinguish between healthy trees and trees with PWD, the decay was determined to round the 40 %. Therefore, if a cure is available, this diagnosis could help to administrate a treatment and reverse the disease evolution.

Hence, the main conclusion of the developed study is that the studied method could be used to assess physiological states of living pine trees, and that the $Z_1/Z_{50}$ impedance parameter could be applied as a risk factor.

## ACKNOWLEDGEMENTS

## REFERENCES

Bauchot, A. D., Harker, F. R. and Arnold, W. M., (2000). The Use of Electrical Impedance Spectroscopy to Assess the Physiological Condition of Kiwifruit. *Postharvest Biology and Technology*, 18 9-18.

Callegaro, L., (2009). The Metrology of Electrical Impedance at High Frequency: a Review. *Meas. Sci. Techno*, 20 022002.

Dean, D. A., Ramanathan, T., Machado, D. and Sundararajan, R., (2008). Electrical Impedance Spectroscopy Study of Biological Tissues. *J Elesctrostat*, 66 (3-4): 165-177.

Dejmek, P. and Miyawaki O., (2002). Relantionship between the Electrical and Rheological Properties of Potato Tuber Tissue after Various Forms of Processing. *Biosci. Biotechnol. Biochem.*, 66 (6), 1218-1223.

Fang, Q., Liu, X. and Cosic, I., (2007). Bioimpedance Study on Four Apple Varieties. *IFMBE Proceedings*, 17, 114-117.

Fukuma, H., Tanaka, K. and Yamaura, I., (2001). Measurement of Impedance of Columnar Botanical Tissue Using the Multielectrode Method. *Electronics and Communications in Japan*, 3, 84, 2.

Giouvanoudi, A. C. and Spyrou N. M., (2008). Epigastric Electrical Impedance for the Quantitative Determination of the Gastric Acidity. *Physiol. Meas.*, 29 1305-1317.

Grimnes, S. and Martinsen, O. (2008). Bioimpedance & Bioelectricity Basics, 2nd Edition. *Academic Press of Elsevier.*

Harker, F. R. and Maindonald, J. H., (1994). Ripening of Nectarine Fruit – Changes in the Cell Wall, Vacuole, and Membranes Detected Using Electrical Impedance Measurements. *Plant Physiol*, 106: 165-171.

Hayashi, T., Todoriki, S., Otobe, K., Sugiyama, J., (1992). Impedance Measuring Technique for Identifying Irradiated Potatoes. *Biosci. Biotechnol. Biochem.*, 56 (12), 1929-1932.

He, C., Zhang, L., Liu, B., Xu, Z. and Zhang, Z., (2008). A Digital Phase-sensitive Detector for Electrical Impedance Tomography. *IEEE proceedings*.

Ivorra, A., (2003). Bioimpedance Monitoring for Physicians: an Overview. *Centre Nacional de Microelectrònica, Biomedical Applications Group*.

Kyle, U. et al., (2004). Bioelectrical Impedance Analysis – Part I: Review of Principles and Methods. *Clinical Nutrition*, 23, 1226-1243.

Pliquett, U., (2010). Bioimpedance: A Review for Food Processing. *Food Eng Rev*, 2:74-94.

Rafiei-Naeini, M., Wright P. and McCann, H., (2007). Low-Noise Measurements for Electrical Impedance Tomography. *IFMBE Proceedings*, 17 324-327.

Repo, T., Zhang, G., Ryyppö, A. and Rikala, R., (2000).

The Electrical Impedance Spectroscopy of Scots Pine (*Pinus sylvestris* L.) Shoots in Relation to Cold Acclimation. *Journal of Experimental Botany*, 51, 353, 2095-2107.

Ross, A. S., Saulnier, G. J., Newell, J. C. and Isaacson, D., (2003). Current Source Design for Electrical Impedance Tomography. *Physiol. Meas.*, 24 509-516.

Saulnier, G. J, Ross, A. S. and Liu, n., (2006). A High-Precision Voltage Source for EIT. *Physiol. Meas.*, 27 S221-S236.

Seoane, F., Bragós, R. and Lindecrantz, K. (2006). Current Source for Multifrequency Broadband Electrical Bioimpedance Spectroscopy Systems. A Novel Approach. *Proceedings of the 28ᵗʰ IEEE*, 1-4244-0033.

Väinöla, A. and Repo, T. (2000). Impedance Spectroscopy in Frost Hardiness Evaluation of *Rhododendron* Leaves. *Annals of Botany*, 86: 799-805.

Vozáry, E. and Mészáros, P., (2007). Effect of Mechanical Stress on Apple Impedance Parameters. *IFMBE Proceedings*, Vol. 17.

Willis, J. and Hobday, A., (2008). Application of Bioelectrical Impedance Analysis as a Method for Estimating Composition and Metabolic Condition of Southern Bluefin Tuna (*Thumus maccoyii*) During Conventional Tagging. *Fisheries Research*, 93 64-71.

Yamamoto, T., Oomura, Y., Nishino, H., Aou, S. and Nakano, Y., (1985). Driven Shield for Multi-Barrel Electrode. *Brain Research Bulletin*, 14 103-104.

Yoo, P. J., Lee, D. H., Oh, T. I. and Woo, E. J., (2010). Wideband Bio-impedance Spectroscopy using Voltage Source and Tetra-polar Electrode Configuration. *Journal of Physics*, 224 012160.